

**Longitudinal intravital imaging of transplanted mesenchymal stem cells elucidates their functional integration and therapeutic potency in an animal model of interstitial cystitis/bladder pain syndrome**

Chae-Min Ryu<sup>1,2,†</sup>, Hwan Yeul Yu<sup>1,2,†</sup>, Hye-Yeon Lee<sup>2,3,†</sup>, Jung-Hyun Shin<sup>1</sup>, Seungun Lee<sup>2,3</sup>, Hyein Ju<sup>2,3</sup>, Bjorn Paulson<sup>4,5</sup>, Sanghwa Lee<sup>5,6</sup>, Sujin Kim<sup>2,3</sup>, Jisun Lim<sup>2,3</sup>, Jinbeom Heo<sup>2,3</sup>, Ki-Sung Hong<sup>7</sup>, Hyung-Min Chung<sup>7,8</sup>, Jun Ki Kim<sup>5,6,\*</sup>, Dong-Myung Shin<sup>2,3,\*</sup>, Myung-Soo Choo<sup>1,\*</sup>

<sup>1</sup>Department of Urology, <sup>2</sup>Department of Biomedical Sciences, <sup>3</sup>Department of Physiology, Asan Medical Center, University of Ulsan College of Medicine, Seoul, Korea, <sup>4</sup>Department of Physics, Yonsei University, Seoul, Korea, <sup>5</sup>Biomedical Engineering Research Center, ASAN Institute for Life Sciences, Asan Medical Center, <sup>6</sup>Department of Convergence Medicine, University of Ulsan, College of Medicine, Seoul, Korea, <sup>7</sup>Department of Stem Cell Biology, School of Medicine, Konkuk University, Seoul, Korea, <sup>8</sup>Mirae Cell Bio Co. Ltd, Seoul, Korea

<sup>†</sup>These authors contributed equally to this work.

**Running title:** Intravital imaging of M-MSCs for treatment of IC/BPS

\* **Correspondence:** Myung-Soo Choo, M.D., Ph.D. ([mschoo@amc.seoul.kr](mailto:mschoo@amc.seoul.kr)), Dong-Myung Shin, Ph.D. ([d0shin03@amc.seoul.kr](mailto:d0shin03@amc.seoul.kr)), Jun Ki Kim, Ph.D. ([kim@amc.seoul.kr](mailto:kim@amc.seoul.kr))

**This Supplementary Material file contains twelve Supplementary Figures, six Supplementary Movies and their legends.**

## SUPPLEMENTARY FIGURE LEGENDS

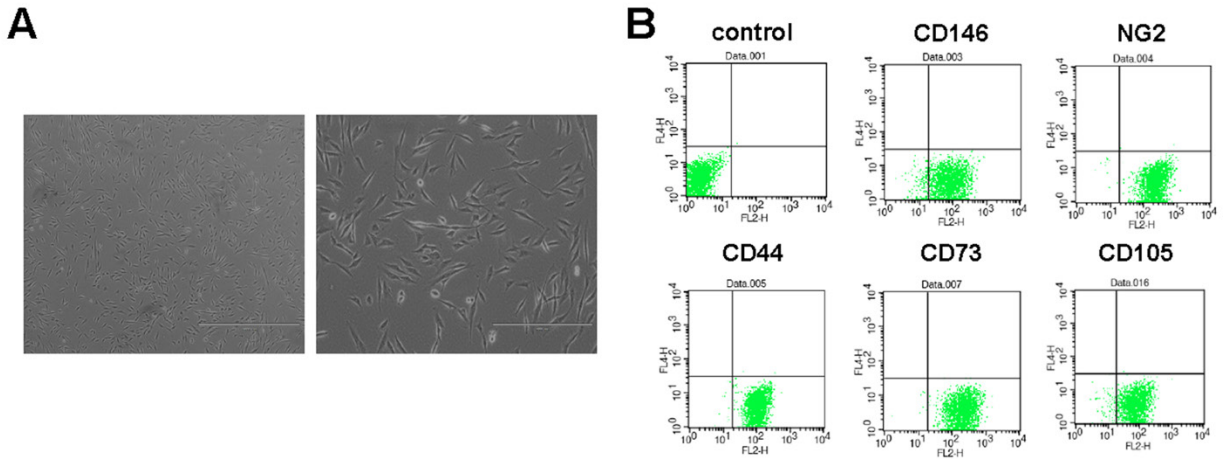


**Figure S1. Characterization of hESC-derived M-MSCs.**

(A) Morphological characterization of M-MSCs (left panel; magnification  $\times 40$ , scale bar = 400  $\mu\text{m}$  and right panel; magnification  $\times 100$ , scale bar = 1,000  $\mu\text{m}$ ). (B) Analysis of surface antigen expression showing that M-MSCs were positive for markers of MSCs (CD44, CD73, and CD105) and pericytes (CD146 and NG2).

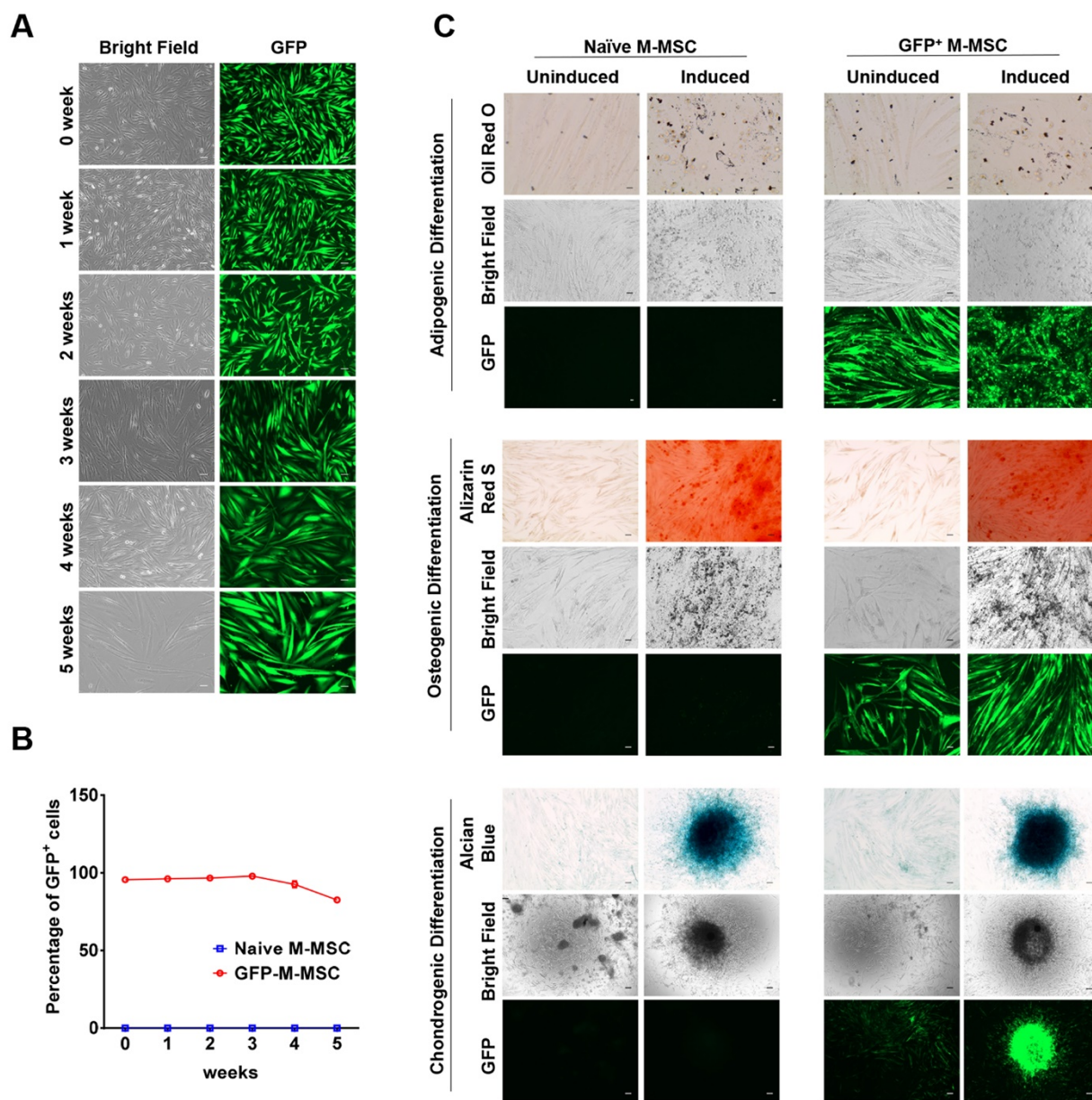


**Figure S2. Stable expression of GFP in GFP<sup>+</sup> M-MSCs.**

Expression of GFP in M-MSCs infected with a lentivirus containing a GFP-expressing cassette during long-term cultivation and multi-lineage differentiation. **(A and B)** Expression of GFP during cultivation of GFP<sup>+</sup> M-MSCs for 5 weeks was monitored using an inverted fluorescence

microscope (A; magnification  $\times 100$ , scale bar = 100  $\mu\text{m}$ ) and by FACS analysis (B). (B) The percentage of GFP-expressing cells determined by FACS analysis was quantified from three independent experiments. Data are presented as the mean  $\pm$  SEM. (C) Expression of GFP during adipogenic (upper panel;  $\times 200$  magnification; scale bar = 20  $\mu\text{m}$ ), osteogenic (middle panel;  $\times 200$  magnification; scale bar = 40  $\mu\text{m}$ ), and chondrogenic (lower panel;  $\times 40$  magnification; scale bar = 200  $\mu\text{m}$ ) differentiation in control (Naïve) and GFP-expressing M-MSCs (GFP<sup>+</sup> M-MSCs). Adipogenic, osteogenic, and chondrogenic differentiation was characterized by Oil Red O, Alizarin Red S, and Alcian Blue staining, respectively.

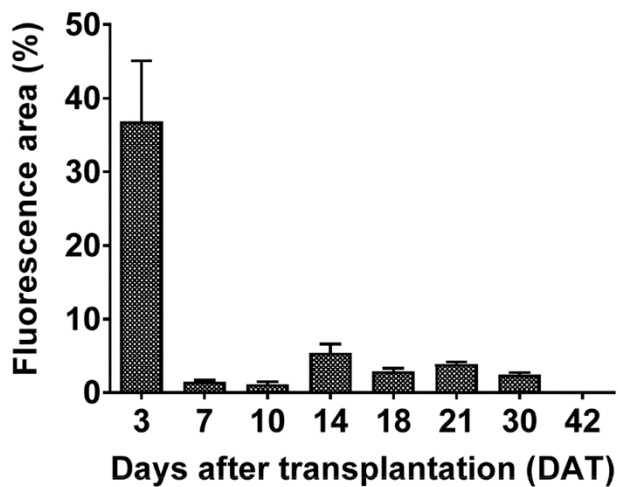


**Figure S3. Quantitative assay of intravital micro-endoscopic imaging**

Percentage of the fluorescent area in confocal endoscopic micrographs. Representative movies obtained in these experiments are available as **Supplementary Movies**.

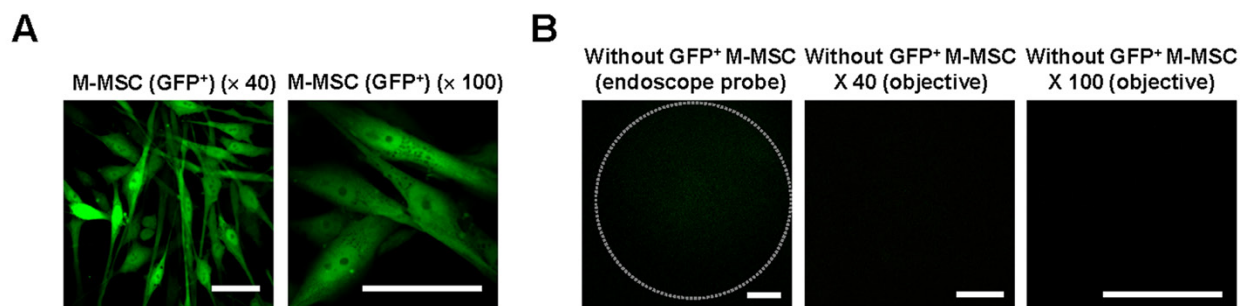


**Figure S4. Low level of autofluorescence in intravital imaging.**

(A) Representative images of GFP in cultured GFP<sup>+</sup> M-MSCs (magnification ×40 and ×100). (B) Longitudinal imaging of living animals not transplanted with GFP<sup>+</sup> M-MSCs. Time-lapse images of the bladders of LPS-IC rats were obtained using a front-view GRIN optical probe endoscopically inserted into the bladder (left, magnification ×40) or an objective lens (middle; magnification ×40, right; magnification ×100). Baseline images from rats not injected with GFP<sup>+</sup> M-MSCs show low autofluorescence, and weak fluorescence signals overall are detected by intravital imaging. Scale bar = 50 μm.

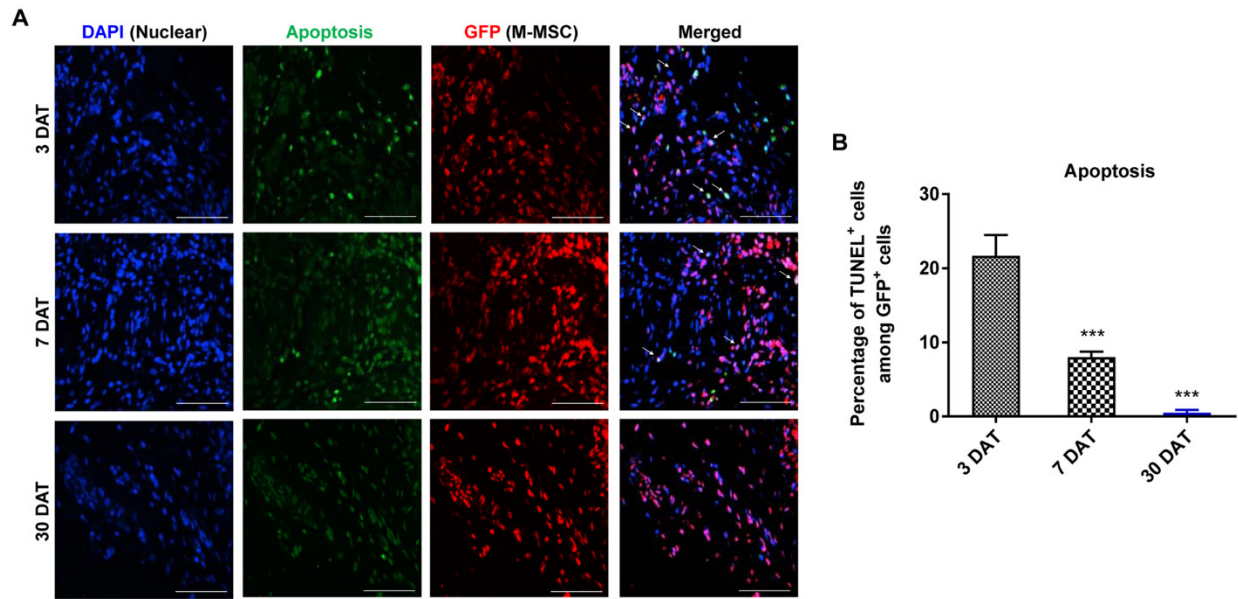


**Figure S5. Apoptosis of transplanted M-MSCs.**

(A) Representative images of staining to detect TUNEL<sup>+</sup> apoptotic cells (red) among transplanted GFP<sup>+</sup> M-MSCs (green) (magnification  $\times 400$ , scale bar = 20  $\mu\text{m}$ ) in bladder tissues of LPS-IC + M-MSC rats at the indicated number of DAT. (B) Quantification of the staining results. Data show the percentage of GFP<sup>+</sup> cells that were TUNEL<sup>+</sup> (n = 8) and are presented as the mean  $\pm$  SEM. \*\*\*p<0.001 compared with the 3 DAT group according to a one-way ANOVA with the Bonferroni post-hoc test.

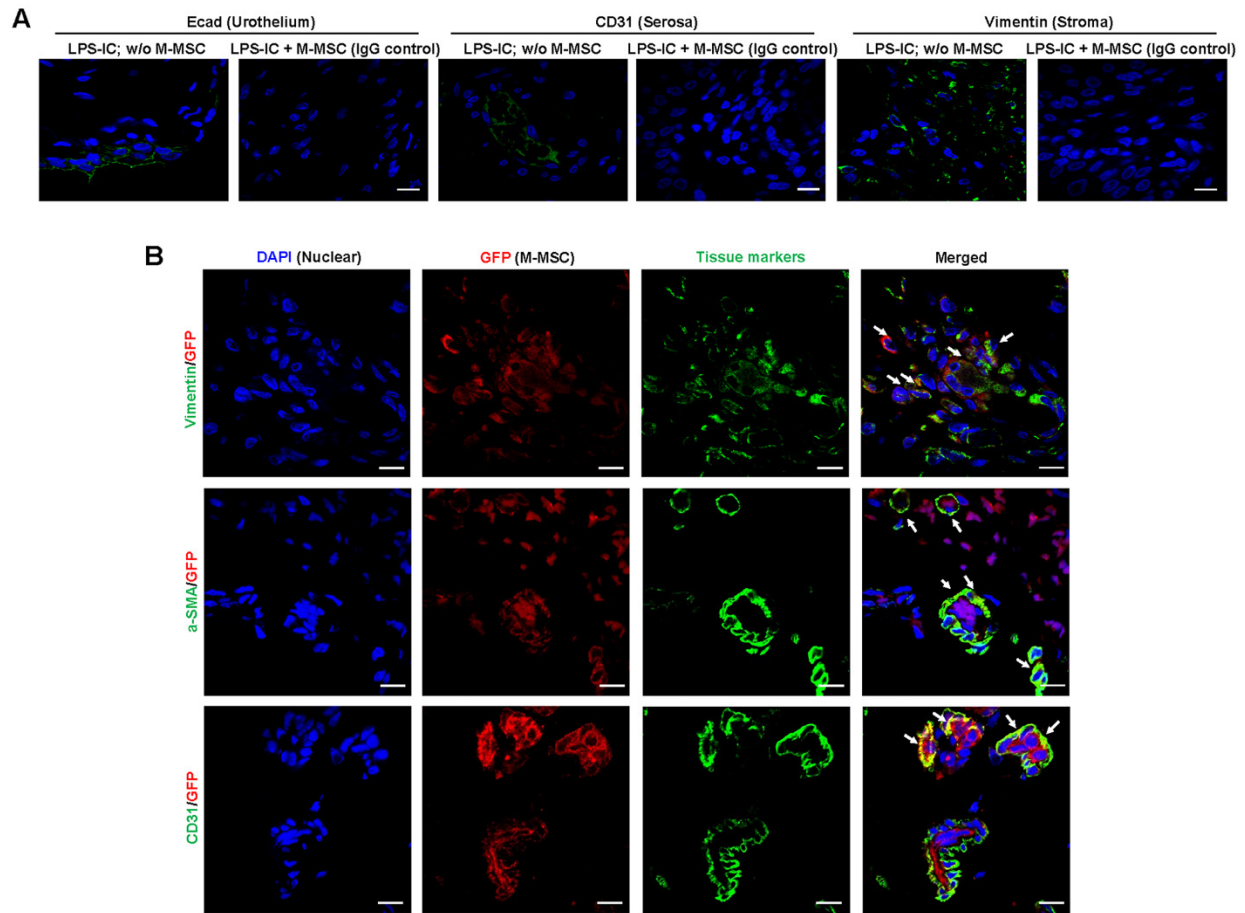


**Figure S6. Immunostaining of transplanted M-MSCs.**

(A) To rule out the possibility of non-specific staining, bladder tissues of LPS-IC + M-MSC rats were co-stained with mouse and rabbit IgG control antibodies, and bladder tissues of LPS-IC rats not injected with M-MSCs (LPS-IC; w/o M-MSC) were co-stained for the indicated markers (green) and GFP (red) (magnification  $\times 1,000$ , scale bar = 10  $\mu\text{m}$ ) as two sets of negative controls.

(B) Representative confocal micrographs of bladder sections of LPS-IC + M-MSC rats stained for GFP (red) and vimentin,  $\alpha$ -SMA, or CD31 (green) at 30 DAT (magnification  $\times 1,000$ , scale bar = 10  $\mu\text{m}$ ). Nuclei were stained with DAPI (blue).

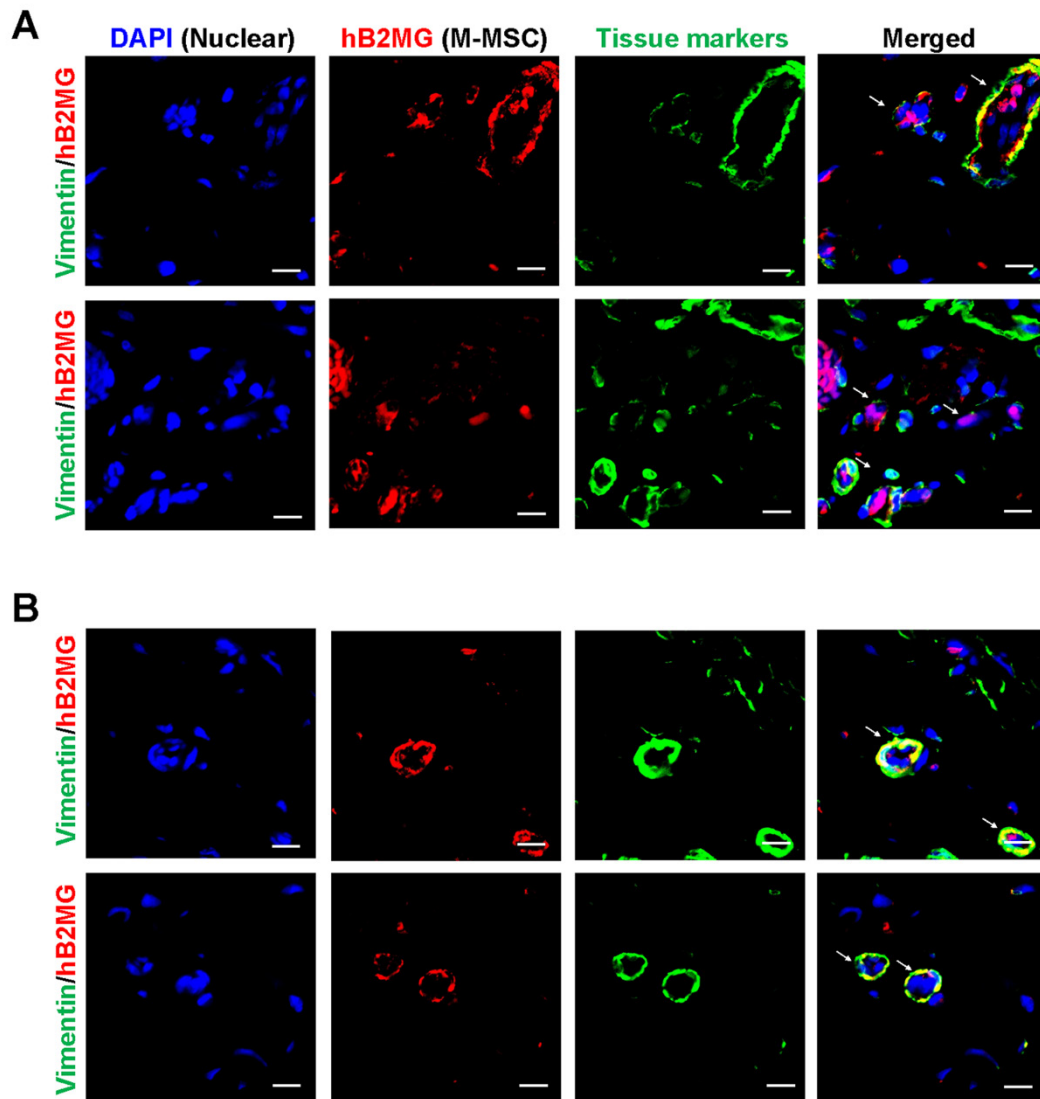


**Figure S7. Co-expression of vimentin and human antigens in transplanted M-MSCs.**

Representative confocal micrographs of bladder sections of LPS-IC + M-MSC rats stained for hB2M (red) and vimentin at 7 DAT (upper panel) and 30 DAT (lower panel) in blood vessel-like structures (magnification  $\times 1,000$ , scale bar = 10  $\mu\text{m}$ ). Nuclei were stained with DAPI (blue).



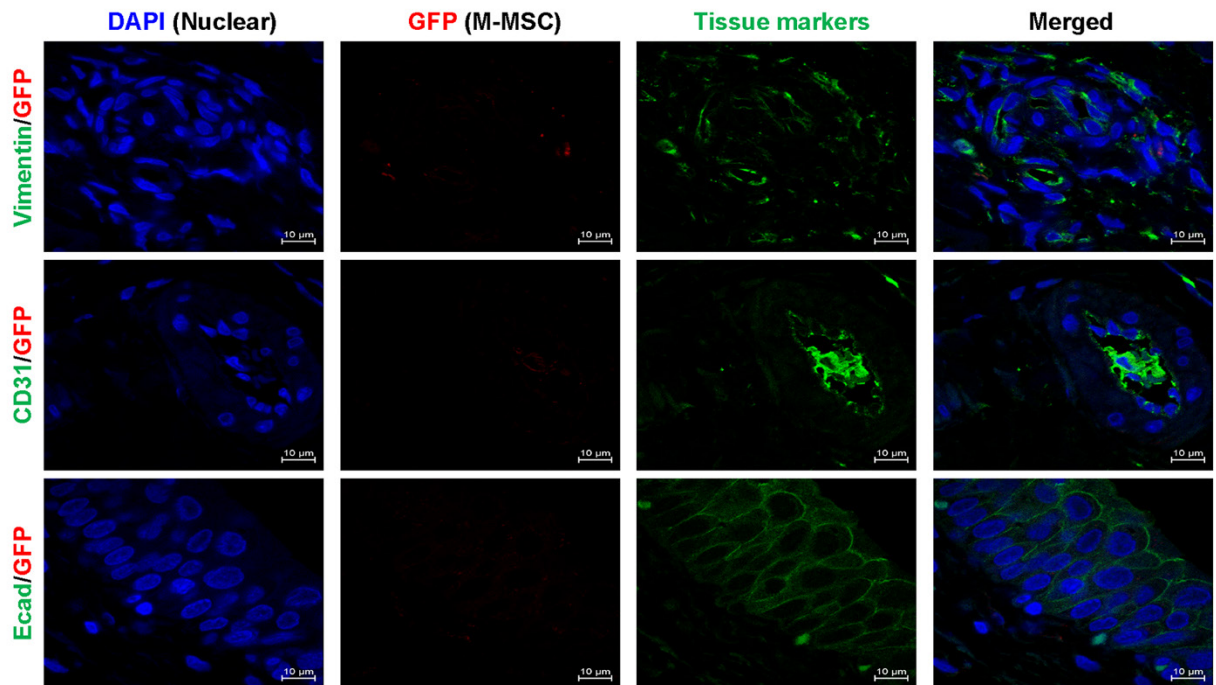


**Figure S8. Disappearance of transplanted M-MSCs at 1 month after transplantation.**

Representative confocal micrographs of bladder sections of LPS-IC + M-MSC rats stained for GFP (red) and vimentin, E-cadherin (Ecad), or CD31 (green) at 42 DAT (magnification  $\times 1,000$ , scale bar = 10  $\mu\text{m}$ ). Nuclei were stained with DAPI (blue).

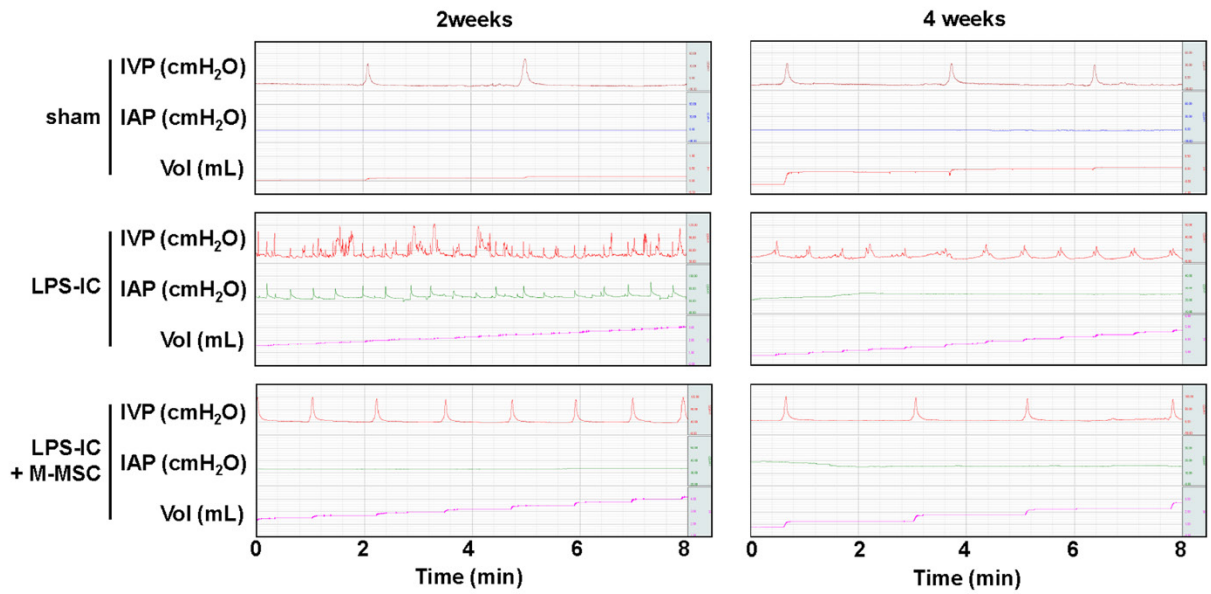


**Figure S9. Long-term therapeutic effects of M-MSCs on bladder function in LPS-IC rats.**

Representative awake cystometry results at 2 weeks (left) and 4 weeks (right) after injection of  $1 \times 10^6$  M-MSCs (LPS-IC + M-MSc) or PBS (LPS-IC) into LPS-IC rats. Sham: sham-operated.

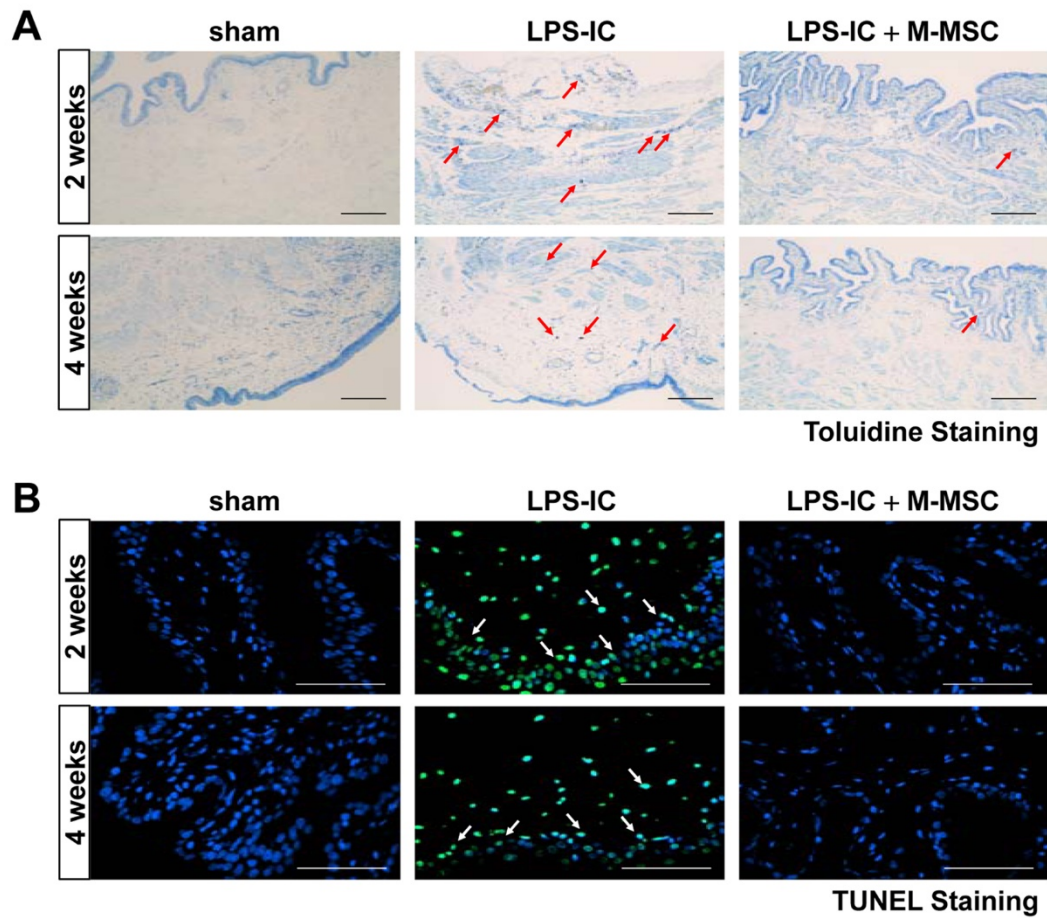


**Figure S10. Therapeutic effects of M-MSCs on chronic bladder injury in LPS-IC rats.**

(**A and B**) Representative Toluidine blue staining (**A**; magnification  $\times 100$ , scale bar = 100  $\mu\text{m}$ ), and TUNEL (**B**; magnification  $\times 400$ , scale bar = 100  $\mu\text{m}$ ) in bladder tissues of LPS-IC rats at 2 and 4 weeks after injection of  $1 \times 10^6$  M-MSCs (LPS-IC + M-MSC) or PBS (LPS-IC). Nuclei were stained with Mayer's hematoxylin (**A**) or DAPI (blue, **B**). Arrows indicate infiltrated mast cells (**A**) and apoptotic cells (**B**). Sham: sham-operated.

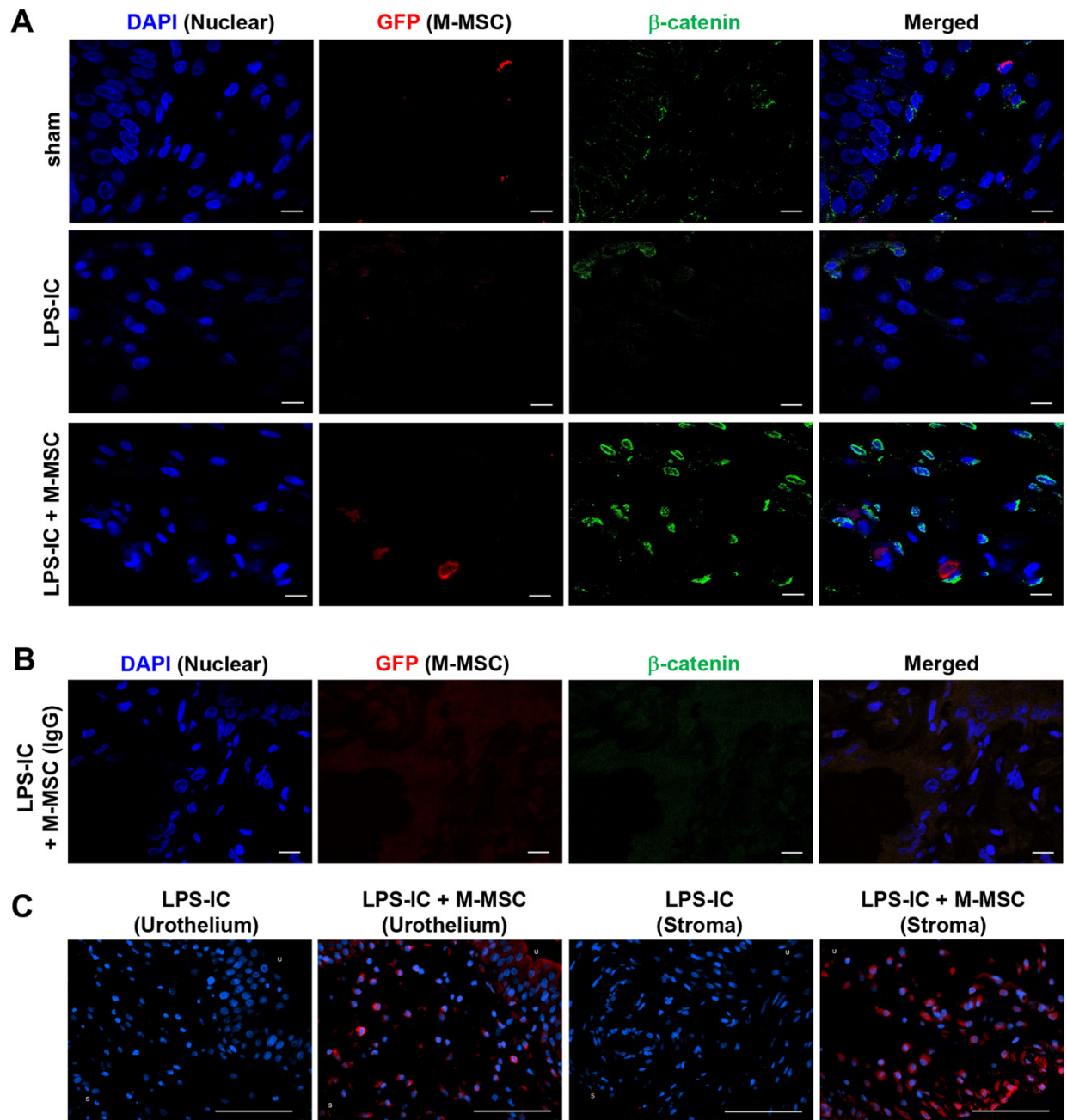


**Figure S11. Immunofluorescence analysis of WNT signaling and engraftment of M-MSCs.**

(A) Representative confocal micrographs of bladder sections from the indicated groups of rats co-stained for GFP (red) and  $\beta$ -catenin (green) (magnification  $\times 1,000$ , scale bar = 10  $\mu\text{m}$ ). Nuclei were stained with DAPI (blue).

(B) Bladder sections of LPS-IC + M-MSC rats were

stained with mouse and rabbit IgG control antibodies as a negative control in experiments assessing the nuclear localization of  $\beta$ -catenin and engraftment of GFP<sup>+</sup> cells (magnification  $\times 1,000$ , scale bar = 10  $\mu\text{m}$ ). **(C)** Bladder tissues of LPS-IC rats not injected with GFP<sup>+</sup> M-MSCs (LPS-IC; w/o M-MSC) were stained as a negative control in experiments assessing the engraftment of GFP<sup>+</sup> cells (magnification  $\times 200$ , scale bar = 200  $\mu\text{m}$ ). Nuclei were stained with DAPI (blue). U: urothelium; S: serosa; sham: sham-operated.

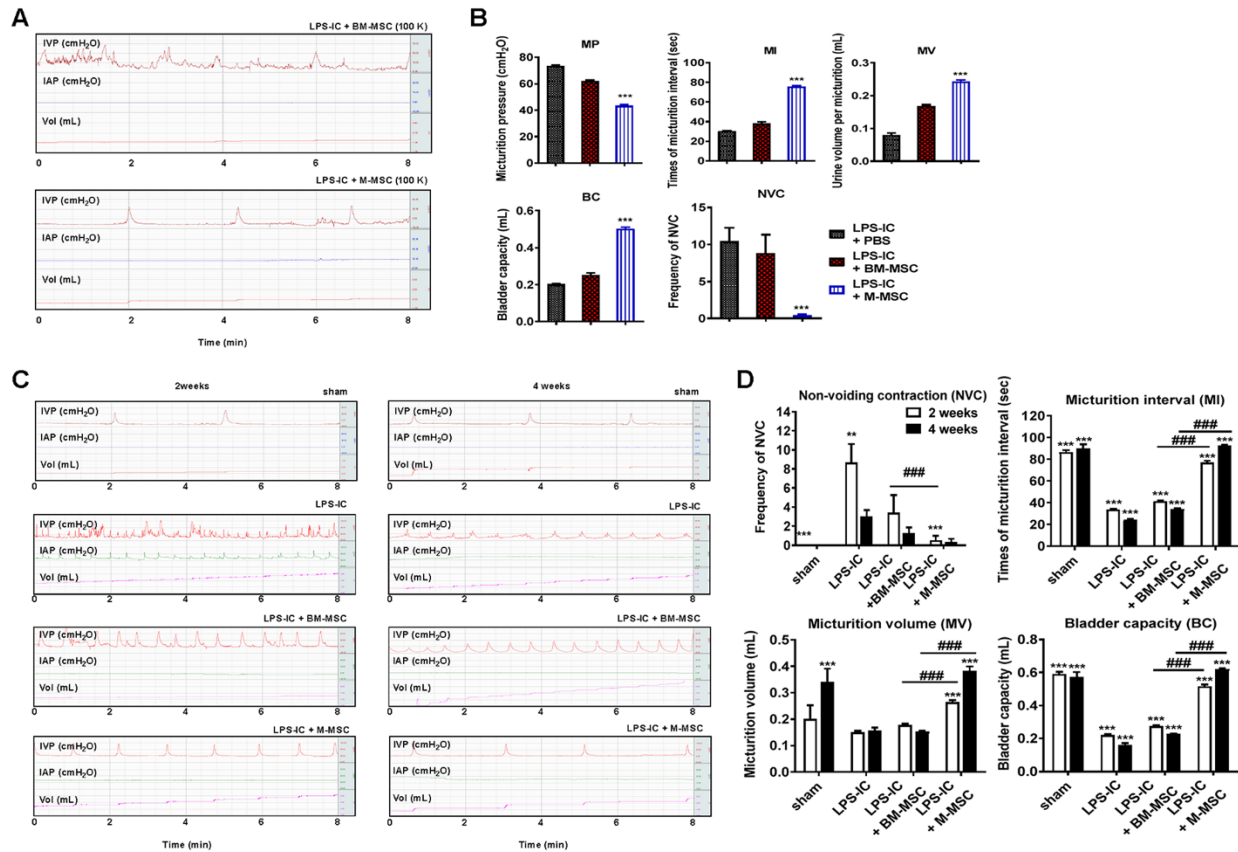


**Figure S12. The therapeutic efficacy of M-MSCs is superior to that of BM-MSCs.**

(A and C) Representative awake cystometry at 1 week (A) or 2 or 4 weeks (C) after injection of M-MSCs or BM-MSCs ( $1 \times 10^5$  cells; 100 K) into the bladders of LPS-IC rats. (B and D) The non-voiding contraction (NVC), micturition interval (MI), micturition volume (MV), and bladder capacity (BC) were quantified from the voiding pattern analysis. All data are presented as the mean  $\pm$  SEM (five independent animals per group). Data were statistically analyzed using a one-way (B) or two-way (D) ANOVA and the Bonferroni post-hoc test. \*\*\* $p < 0.001$  compared with the LPS-IC group; #### $p < 0.001$  for the M-MSC vs. BM-MSC groups.

## **SUPPLEMENTARY MOVIES AND LEGENDS**

**Movie S1.** Intravital endoscope imaging at 3 DAT (**Figure 2**)

**Movie S2.** Intravital endoscope imaging at 30 DAT (**Figure 2**)

**Movie S3.** Intravital microscope 3 DAT with 40×magnification (**Figure 3A**)

**Movie S4.** Intravital microscope 3 DAT with 100×magnification (**Figure 3B**)

**Movie S5.** Intravital microscope 30 DAT with 40×magnification (**Figure 3A**)

**Movie S6.** Intravital microscope 30 DAT with 100×magnification (**Figure 3B**)

**Supplementary Movies** at other days after transplantation would be available at website.

**These videoclips can be also freely downloaded from FTP server (<ftp://sdmlab.iptime.org>).**

**The login ID and password are is “ID: FTP\_Guest and PW: Guest1”.**